NASA TECHNICAL MEMORANDUM

NASA TM X-71531

NASA TM X-71531

SURFACE TOPOGRAPHICAL EFFECTS ON THE STRUCTURAL GROWTH OF THICK SPUTTERED METAL AND ALLOY COATINGS

by T. Spalvins and W. A. Brainard
Lewis Research Center
Cleveland, Ohio 44135

TECHNICAL PAPER proposed for presentation at
Seventeenth Technical Conference of the Society
of Vacuum Coaters
Detroit, Michigan, May 1-2, 1974.

SURFACE TOPOGRAPHICAL EFFECTS ON THE STRUCTURAL GROWTH OF THICK SPUTTERED METAL AND ALLOY COATINGS

by T. Spalvins and W. A. Brainard

Lewis Research Center
Cleveland, Ohio 44135

E-7655

SUMMARY

Thick sputtered S-Monel, silver, and 304 stainless steel coatings were deposited on mica and metal substrates with various surface finishes to investigate the structural growth of the coating by scanning electron microscopy. The geometry and the surface structure of the nodules are characterized. Compositional changes within the coating were analyzed by X-ray dispersion microscopy. Defects in the surface finish (i.e., scratches, inclusions, etc.) act as preferential nucleation sites and form isolated and complex nodules and various surface overgrowths in the coating. The nodule boundaries are very vulnerable to chemical etching and these nodules do not disappear after full annealing. Further, they have undesirable effects on mechanical properties; cracks are initiated at the nodules when the coating is stressed by mechanical forces. These effects are illustrated by micrographs. Nodular growth within a coating can be minimized or eliminated by reducing the surface roughness.

INTRODUCTION

With the achievement of high sputter deposition rates, up to 250 μm/HR (10 mils/HR) increased commercial interest has developed in

thick sputtered deposits. Sputter deposits of thicknesses to 0.63 cm (0.25 in.) have been deposited. Sputtering techniques are presently developed for fabrication of free standing shapes such as foil, sheet, tubing and inner and outer cylindrical structures for thrust chambers.

With the commercial fabrication of thick sputtered deposits, the understanding of the structural growth becomes important. A very limited number of studies have been reported relative to the structural growth of thick sputtered deposits (refs. 1, 2). It has been observed that various crystal features are formed in the deposit matrix during the sputtering process. The most commonly observed feature is a nodular growth type which generally presents an unacceptable condition. These crystallographic features are formed within the columnar structure which are also projected to the surface. This nodular growth has been also observed in thick coatings deposited by electroplating (ref. 3). Many of the growth features for the sputtered coatings are similar to those for electroplated coatings.

It is well known, that not only the physical, electrical and magnetic properties but also the mechanical properties such as strength, toughness and ductility are strongly influenced by the coating microstructure. Therefore, a controlled structural growth should be maintained during the deposition process. It should, however, be realized that the sputtered coatings grow in a complex environment. Factors which generally affect coating formation during sputtering are (1) kinetic energy of the sputtered species, (2) plasma conditions, (3) substrate temperature, (4) surface topography, and (5) specimen

potential. Since the surface is the starting point for coating growth, surface conditions (roughness, inhomogeneities, impurities) have a direct effect on film structure. Inhomogeneities, impurities, steps, ledges etc. are favorable sites for nucleation. Dislocations, surface point defects generally limit the best surface achievable, therefore it is impossible to prepare a metallic surface which is atomically smooth over an appreciable area.

The objective of this study was to examine the substrate effects on the microstructure of thick sputtered metallic coatings by scanning electron microscopy. The influence of annealing, chemical etching and mechanical forces on these coatings was also examined. The thick sputtered coatings (12.5 - 50 μm) were S-Monel, 304 stainless steel and silver. The substrates were mica and polished and sanded bronze surfaces.

APPARATUS AND PROCEDURE

The sputtering apparatus used in this study was a radiofrequency-diode system with a superimposed direct-current bias, as shown in figure 1. This apparatus is described in references 4 and 5. The sputtering targets were a 12.7-centimeter-diameter S-Monel, (composition in percent: nickel, 63; copper, 30; iron, 2; manganese, 0.5; silicon, 4; carbon, 0.1), 304 stainless steel and silver disks. The sputtering conditions were kept constant with a radiofrequency power density of 3.5 watts per square centimeter at 7 megahertz and an argon pressure of 20 millitorr. The specimen during the deposition was maintained at ground potential relative to the target. The substrates used

were freshly cleaved mica, bronze, and copper. The metal specimens were (2 by 2 by 0.025 cm) sheets with various surface finishes. These consisted of (1) lapping on a polishing wheel with a resultant surface finish of 5×10^{-2} micrometer (2 μin.), (2) grinding on a 600 grit emery paper with a resultant surface finish of 22.5×10^{-2} micrometer (9 μin.), and (3) sandblasting. Prior to sputter deposition, all metal surfaces were direct-current-sputter-cleaned for about 10 minutes. The distance between the target and the specimen was 2.5 centimeters. A Chromel-Alumel thermocouple was imbedded in the specimen, and the temperature was maintained at 145° C. Coating thicknesses ranged from 12.5 to 50 micrometers (0.5 to 2 mils). The surface topography and the cross section of the coatings were examined by SEM, and the chemical composition was determined by X-ray dispersion microscopy.

RESULTS AND DISCUSSION

Characterization of Sputtered S-Monel 304 Stainless Steel and Silver Coatings by Scanning Electron Microscopy

Examination of sputtered S-Monel, 304 stainless steel and silver coatings on metal and mica surfaces by scanning electron microscopy showed the formation of isolated and fused nodules in the coating matrix. Typical SEM micrographs in figure 2 show the surface view and fracture cross sections of the coating with the nodules. It was observed that the frequency of distribution and size of the nodules changed from sample to sample, while the sputtering conditions remained constant. As shown in figure 2 all the nodules, regardless of their

size, had a cone shape. These micrographs illustrate that nodular growth does not always start at the substrate surface, but can also start during the sputtering process within the deposit. This possibility can be mainly attributed to the sputtering conditions, especially to impurities and coating defects in the sputtered deposit. The size and shape of the individual nodules stemming from each nucleus depend on the size and spacing of the various nuclei (ref. 3).

Geometrical construction of the nodule.- A typical nodule is constructed as shown in figure 3. The surface of the nodule is a circular arc, and it projects above the surface by a distance h. The diameter of the nodule d increases as the film thickness t increases. The boundary of the nodule is parabolic in shape, which indicates an ever-increasing size with continuing deposition. These nodules have a tendency to grow in size with an increase in film thickness.

The diameter and height to some extent is directly dependent upon the coating thickness. A typical size of the largest nodule for a sputtered silver coating of 50 μm (2 mills) thick is about 23 μm in diameter and about 6 μm in height above the matrix surface. Under the sputtering conditions selected for this study the nodular diameter was 50 percent of the coating thickness.

Surface characterization of nodules.- The final growth form of the nodules has a structure of various polyhedral crystallites as shown in figures 4 and 5. The shape of the crystallites change from a polyhedral type for the sputtered silver deposits in figure 4 to a more prismatic type for sputtered 304 stainless steel in figure 5. In both instances

the crystallites are aligned in the direction of the sputtering target. The crystallites of the sputtered silver are on the average 3.5 μm in width whereas the crystallites for the 304 stainless steel are about 0.5 μm. Sputtered alloy coatings as would be expected tend to form finer crystallites than pure elemental metals.

In both instances the individual crystallites appear to be loosely bounded and this can be distinctly seen at the higher magnifications. Another feature which is very obvious from these micrographs is the distinct separation at the mismatch boundary between the nodule and the matrix.

Surface roughness effects on coating structure.- The onset of nodular growth as seen in figure 2 can be attributed to the substrate effects and the sputtering conditions. In order to establish the nature of deposit growth on surfaces, very smooth surfaces were selected. Freshly cleaved mica sheets were selected as substrates. The film structure of S-Monel formed on mica was examined by SEM and a typical cross section of the deposit is shown in figure 6. These deposits have a uniform columnar structure without nodular growth. Figure 7 shows the structural growth of sputtered silver on mica with a cleavage step. The surface defect such as a step or ledge acts as a preferential nucleation site. As a result a nodular growth pattern is formed. These preferential nucleation sites exhibit an increased growth rate with respect to the smooth surface.

Metallic surfaces of brass and copper with different surface roughnesses were used to investigate topographical effects on structural

growth. Figure 8 shows a surface of S-Monel coating sputtered on a brass specimen where one section was highly polished (to 5×10^{-2} μm; 2 μin.) and the other section was sandblasted. The figure reveals a distinct difference in the coating topography due to the surface roughness effects which are transmitted through the coating. The coating on the sandblasted section of the specimen shows considerable roughness with a high concentration of nodules. The coating on the polished section shows a featureless surface structure. Figure 9 shows surface view of a sputtered coating on a brass substrate sanded with a 600 grit abrasive paper to a surface finish of 22.5×10^{-2} micrometer (9 μin.). The nodules have a tendency to form preferentially in high concentrations along the edge boundaries of the scratches, which are favorable sites for nucleation. A high degree of nodule overlapping or partial fusion is also seen at these locations.

Annealing effects on coating structure.- As surface roughness increases, residual stresses also increase. These stresses may act as nucleation inducers to increase nucleation rates and the subsequent growth of nodules. To determine the influence of surface residual stress effects produced during sanding on nodular growth, the sanded specimens were completely annealed (at 810° to 870° C) before the coating was sputter-deposited. A surface micrograph of one of the specimens with this sputtered coating is shown in figure 10. The film retains the nodular growth. This result implies that the surface stresses are not the primary contributing factors for the nodular growth.

Another approach was taken to determine the effect of postdeposition annealing on the behavior of these nodules. It was found that after full annealing in vacuum at temperatures of 870° C the nodules did not change or disappear, as shown in figure 11. The only observable change is the surface faceting caused by the high temperature.

From figures 10 and 11 it appears that nodular growth is associated with surface defects rather than surface stresses. Nucleation studies of vapor-deposited films reveal (ref. 6) that nucleation is indeed favored at steps or ledges on the surface and suggest that the nucleation rate is also influenced at these sites. For instance, the scratch edges inclined at various angles to the flat portion of the crystal exhibit different nucleation rates and subsequent grain growth. It is interesting to note that the growth from the edges of the depressions overtakes growth from the bottoms of the depressions and prevents continuation of growth from the latter regions (ref. 7).

Chemical analysis of S-Monel coating.- X-ray dispersion micromaps were taken of the coating matrix and nodule. No composition changes were detected in S-Monel. These results indicated that the sputtered S-Monel coating had uniform composition distribution.

CHEMICAL ETCHING EFFECTS

As previously shown, the surface structure of the nodules consists of loosely bounded polyhedrons, and also the nodule itself has a very distinct mismatch boundary with the matrix. These distinct boundary disregistries are high energy sites and therefore would be expected to be more vulnerable to chemical attack than rest of the matrix. The

following micrographs in figures 12, 13 and 14 show the chemical etching effects on the nodules and their boundaries. The silver and S-Monel deposits were etched with dilute HNO_3. Figure 12 shows the surface disintegration of the sputtered S-Monel nodule along the boundary lines. The surface vacancy is shown in figure 13 where the top of the nodule has fallen out. After more extensive etching the nodule can be completely removed, thus leaving a hole in the coating as seen in figure 14.

COMPLEX SURFACE OUTGROWTHS

In addition to the individual nodular growth, more complicated structural growths are formed on coatings, as shown in figures 15 and 16. Substrate defects, inhomogeneities, or impurities are believed to be the cause for extreme localized growth. The very common surface growth shown in figure 15 is a result of the interference of adjacent nodules during the growth process. Certain nodules have a preferential growth and thus effectively overwhelm their neighbors and form a cauliflower structure. The basic mechanism for this type of growth formation is not clear, but it is possible that the primary nodules when formed are subnucleating and thus produce this cauliflower structure. Figure 16 shows a wormlike surface growth at two magnifications.

EFFECT OF NODULAR STRUCTURE ON FRACTURE CHARACTERISTICS

It was observed that, when a nodule reaches a critical diameter on the surface and when the film is exposed to mechanical forces such as bending, the coating will have a tendency to break around the nodule edges (fig. 17), but not through the nodule. The cross sectional view

of the nodule in figure 18 shows crack formation around the nodule boundary and as a result cracking in the coating below the nodule. The nodule as seen in figure 18 exerts localized stresses in the coating and thus acts as source for crack initiation. The nodule can simply be ejected from its place and leave an empty cavity, as shown in figure 19. The size of the nodules has an apparent effect on the mechanical properties. As the coating thickness increases, the size of the nodule also increases. For thin films the nodules are very small and their effects are less detrimental. Bending tests show that strict control should be exercised in obtaining the desired structure by carefully preparing the surface finish before sputter deposition in order to avoid surface defects and imperfections which serve to nucleate nodule formation.

SUMMARY OF RESULTS

The structural growth of thick S-Monel, 304 stainless steel, and silver coatings sputtered at constant sputtering conditions on surfaces with various finishes was evaluated by scanning electron microscopy and X-ray dispersion microscopy. Annealing, chemical etching, and bending experiments were also performed on these coatings. The following results were obtained from this investigation:

1. On smooth mica, and highly polished (5×10^{-2} μm; 2 μin.) metallic surfaces, the sputtered coating had a columnar structure.

2. Surface defects (scratches, inclusions, impurities, etc) on metals acted as preferential nucleation sites and as a result isolated nodules, complex nodular type structures, and various surface overgrowths

were formed. The size of the nodules increased as the thickness of the coating increased.

3. The surface structure of the nodules consists of loosely bound polyhedral crystallites.

4. The nodules within the deposit did not disappear after full annealing.

5. Chemical etching severely attacks the mismatch boundaries between the nodule and the matrix.

6. Nodules and complex surface overgrowths in the coating had undesirable effects on mechanical properties, since they acted as stress raisers and initiated cracks.

7. The coating material did not affect nodular formation. Nodular growth was observed with elemental metals and with complex alloys.

8. No compositional changes were observed inside or outside the nodules in sputtered S-Monel coatings.

9. Nodular growth can be minimized or eliminated by reducing the surface roughness.

REFERENCES

1. Mattox, D. M.; and Kominiak, G. J.: Structure Modification by Ion Bombardment During Deposition. Jour. Vac. Sci. Technol., vol. 9, no. 1, Jan. -Feb. 1972, pp. 528-532.

2. Thornton, John A.. Sputter Coating - Its Principles and Potential. Paper 730544, SAE, May 1973.

3. Gabe, D. R.. Dendritic Growth During Electrodeposition. Metallurgist Materials Technol., vol. 5, no. 2, Feb. 1973, pp. 72-77.

4. Spalvins, Talwaldis: Lubrication With Sputtered MoS_2 Films. Proceedings of the First International Conference on Solid Lubrication. ASLE SP-3, 1971, pp. 360-370.

5. Spalvins, T.. Sputtering - A Vacuum Deposition Method for Coating Material. Paper 72-DE-37, ASME, May 1972.

6. Neugebauer, Constantine A.. Condensation, Nucleation, and Growth of Thin Film Films. Ch. 3 in Handbook of Thin Film Technology, Leon I. Maissel and Reinhard Glang, eds., Mc-Graw-Hill Book Co., Inc., 1970.

7. Assour, Jacques M.. Identification of Chemical Constituents of Defects in Silicon. Jour. Electrochem. Soc., vol. 119, no. 9, Sept. 1972, pp. 1270-1272.

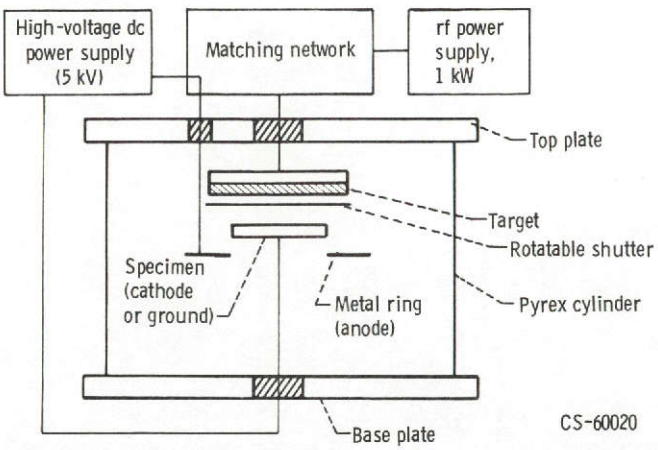

(a) Schematic diagram.

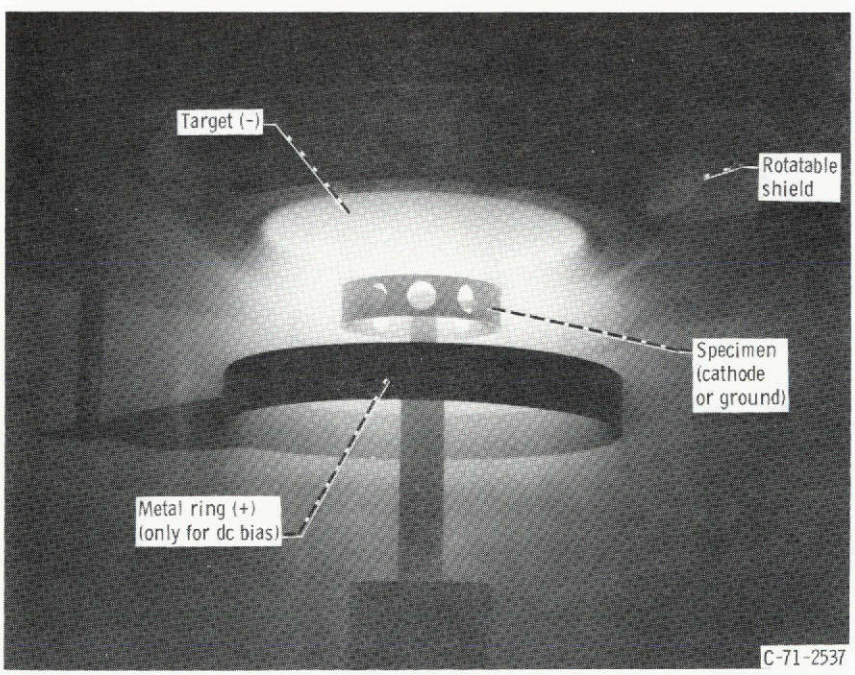

(b) View of apparatus during sputter coating.

Figure 1. - Radiofrequency diode sputtering apparatus with direct-current bias.

E-7655

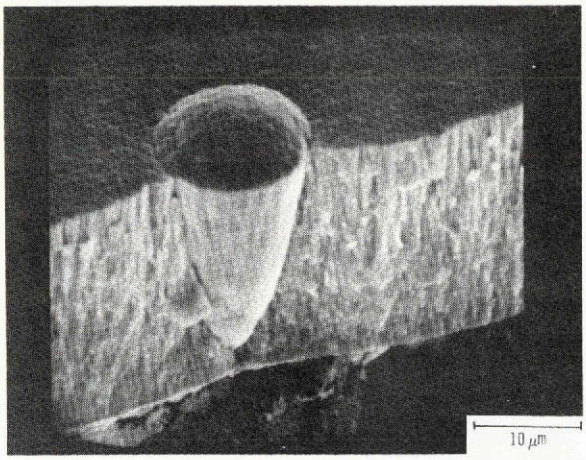

(a) Isolated nodule.

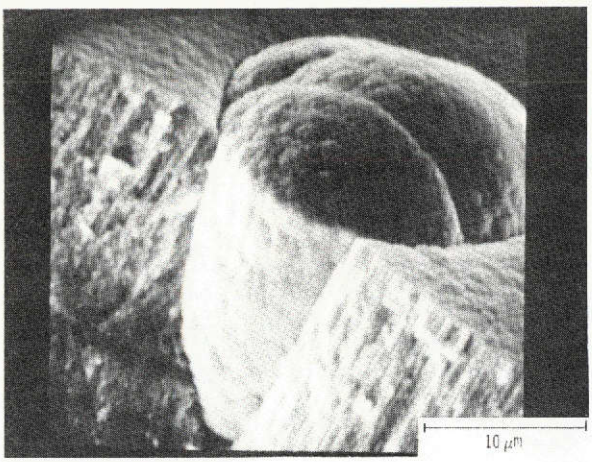

(b) Fused nodules.

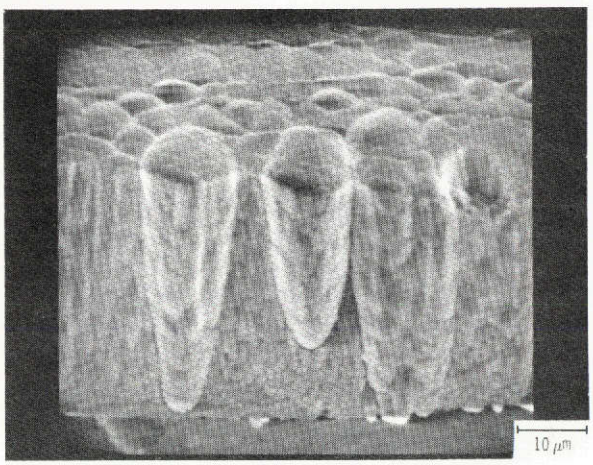

(c) Cluster of nodules.

Figure 2. - Fracture cross sections of nodular growth in S-Monel on brass.

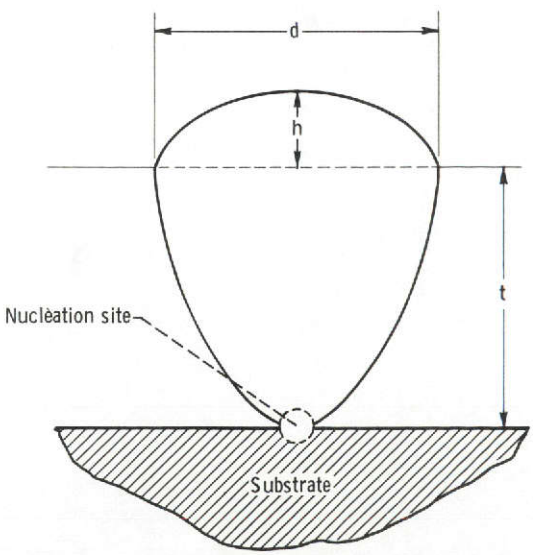

Figure 3. - Geometric construction of typical isolated nodule. Film thickness, t; diameter of nodule, d; height of nodule above surface, h.

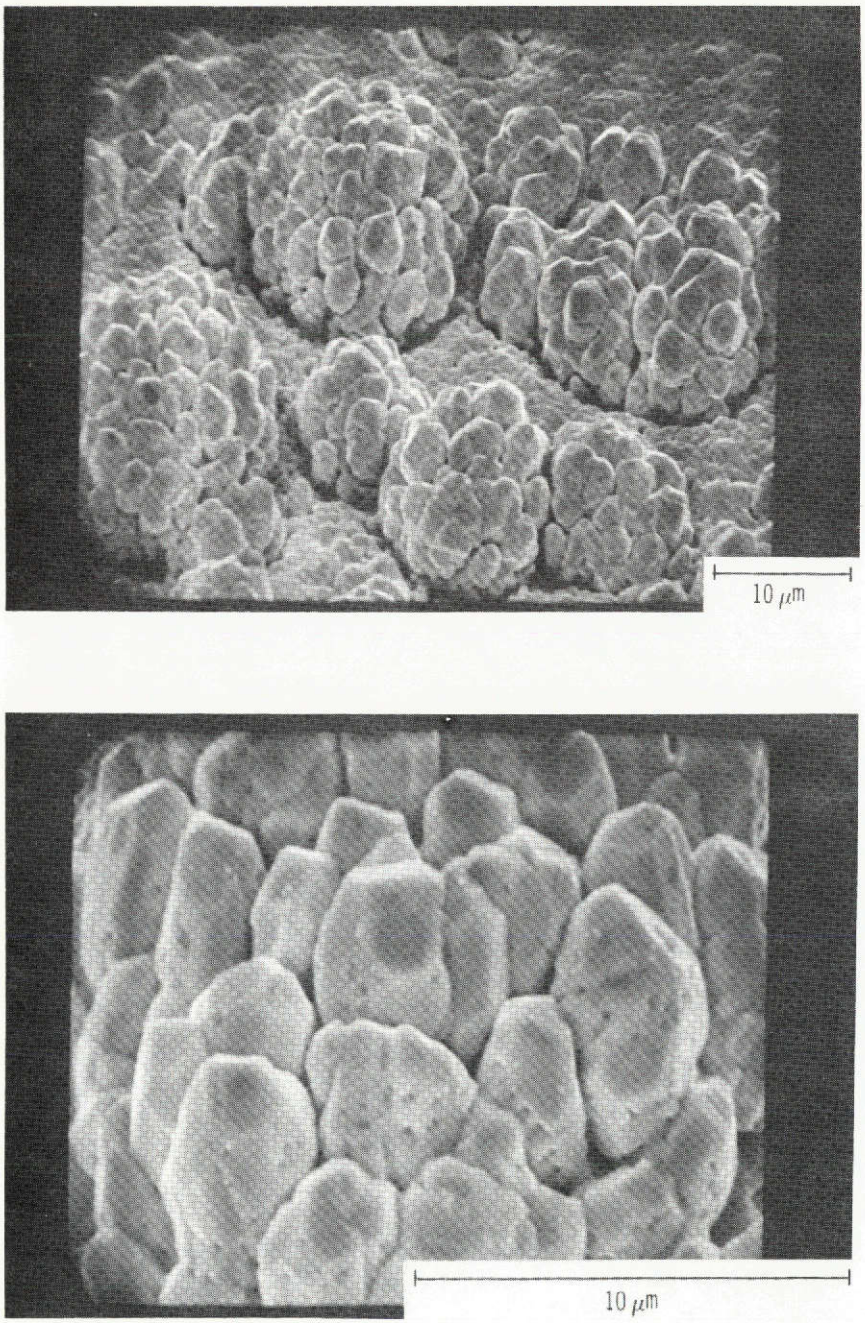

Figure 4. - Surface structure of sputtered silver on brass.

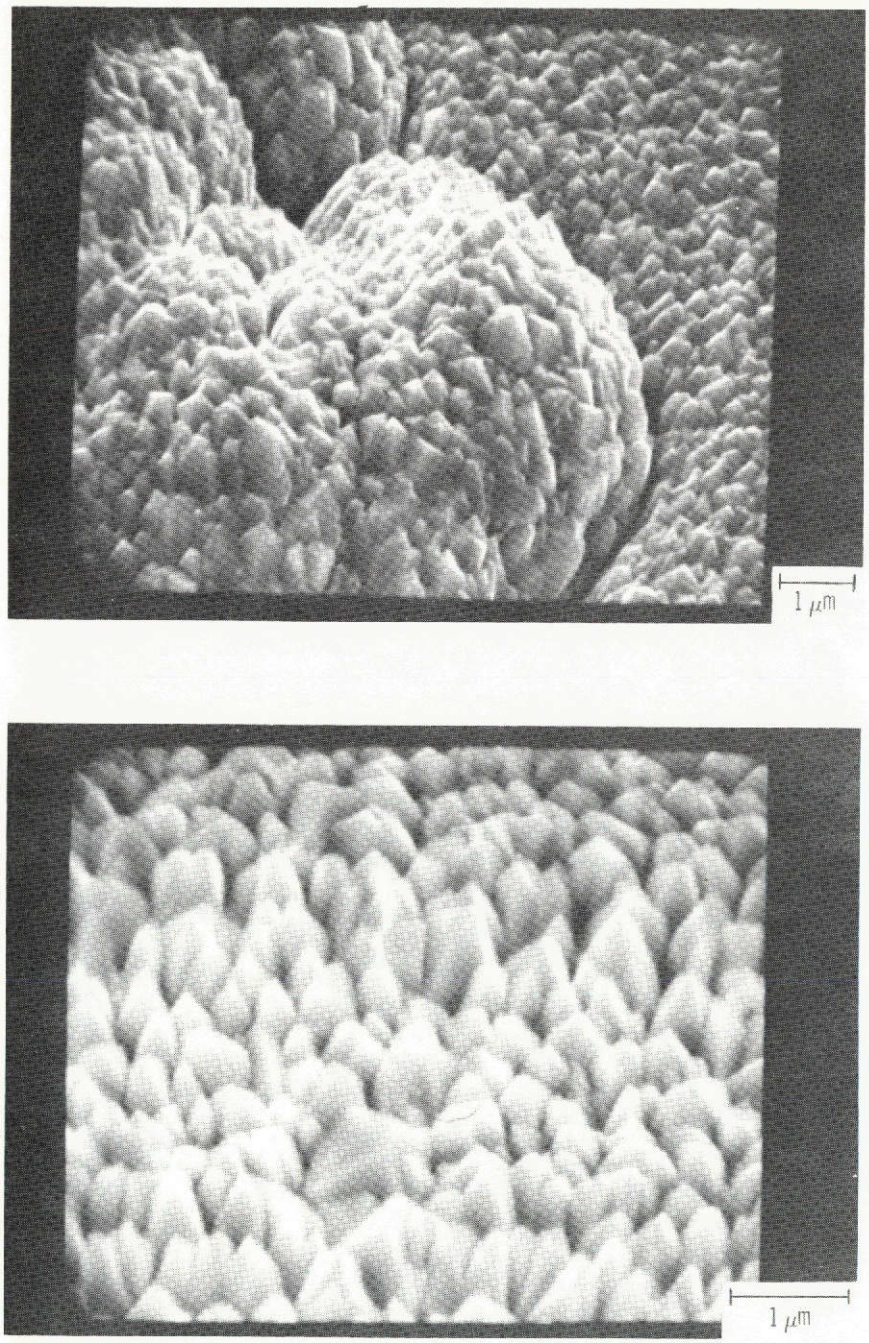

Figure 5. - Surface structure of sputtered 304 stainless steel on brass.

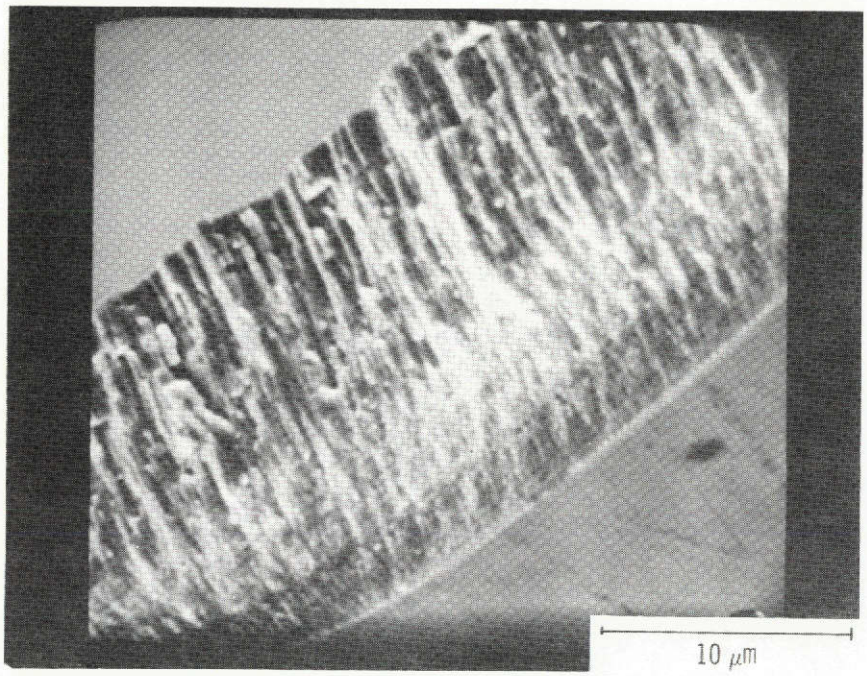

Figure 6. - Typical cross section of sputtered S-Monel on mica.

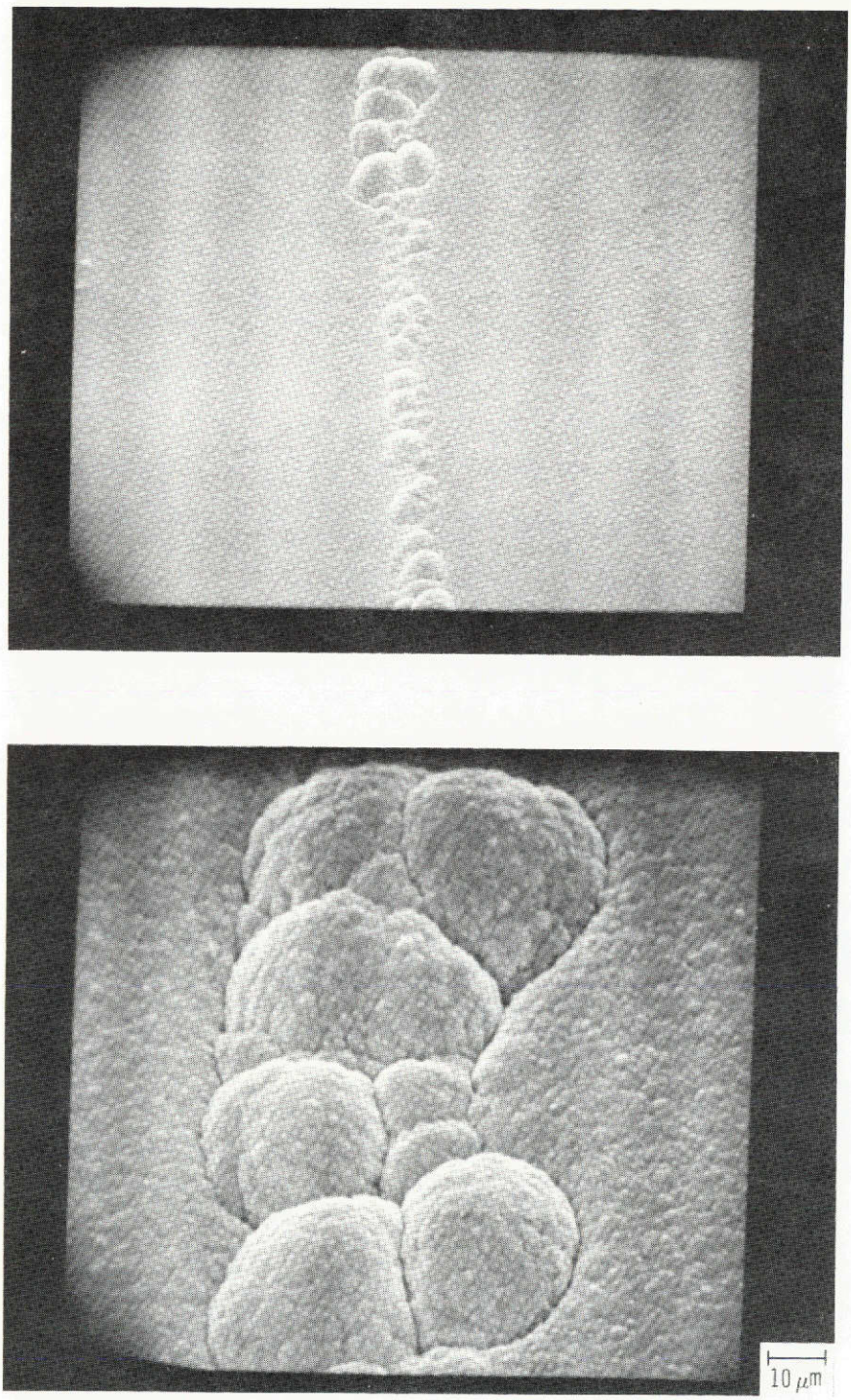

Figure 7. - Surface view of sputtered S-Monel on mica with a cleavage step.

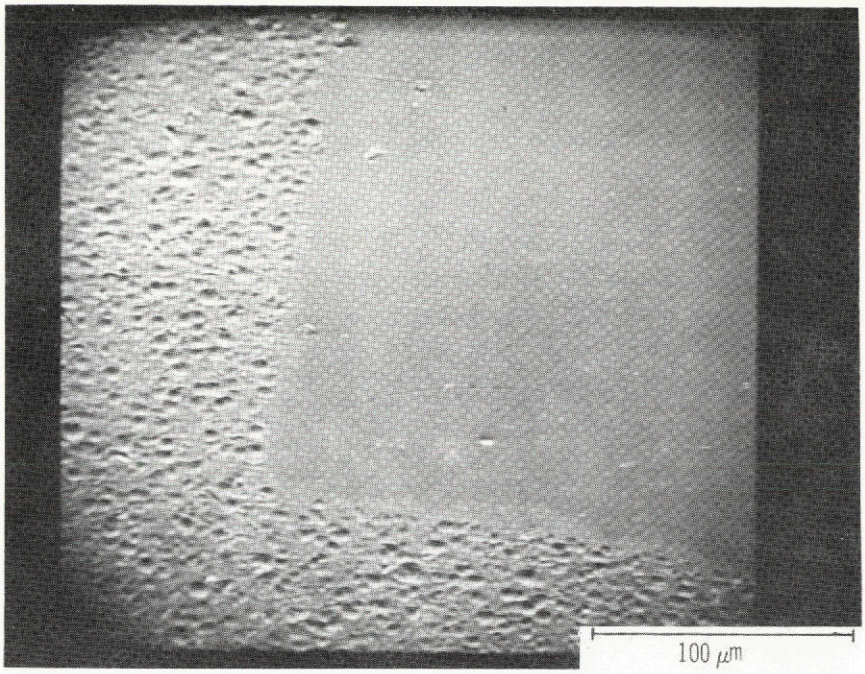

Figure 8. - Surface of sputtered S-Monel coating on smooth and sandblasted sections of brass surface.

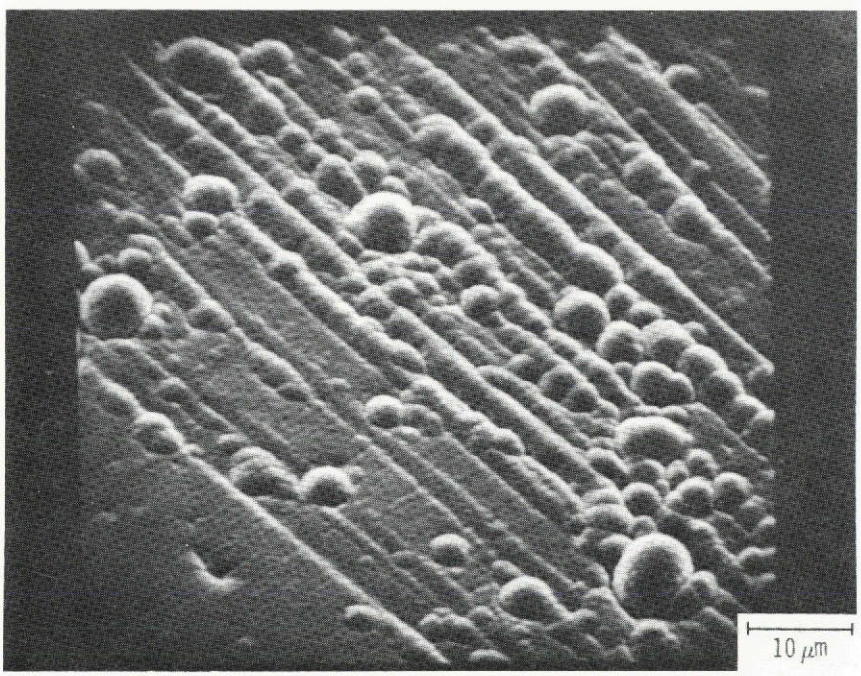

Figure 9. - Surface of sputtered S-Monel on brass surface sanded to 22.5×10^{-2}-micrometer finish.

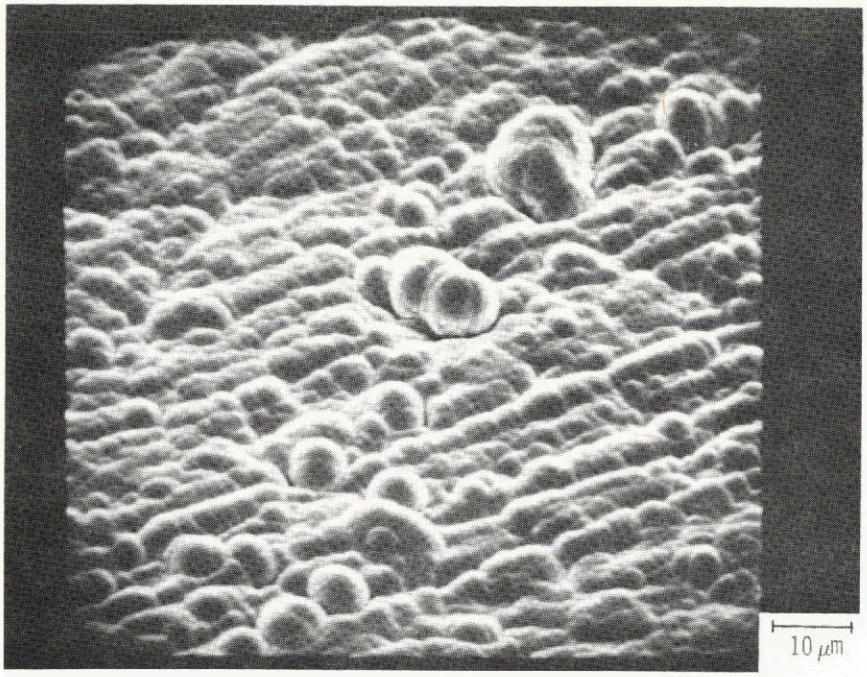

Figure 10. - Surface of sputtered S-Monel on brass surface sanded to 22.5×10^{-2}-micrometer finish and subsequently annealed at 870° C before deposition.

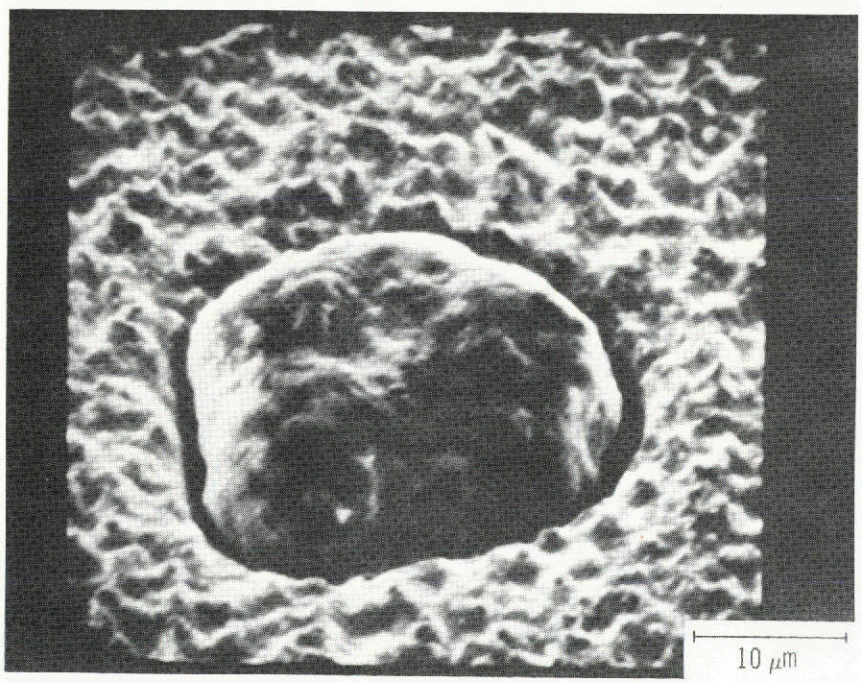

Figure 11. - Surface of sputtered S-Monel on brass after full annealing at 870° C in vacuum.

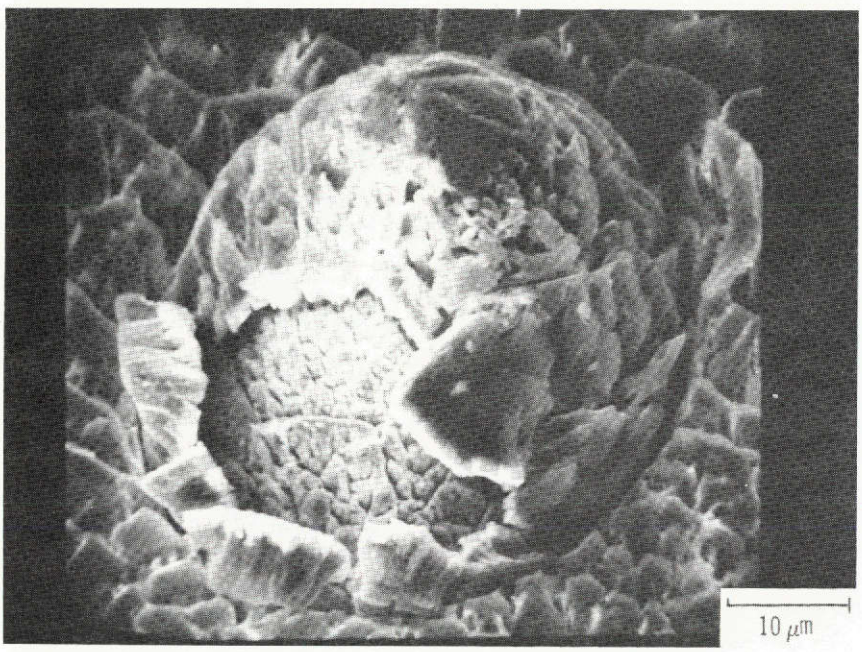

Figure 12. - Disintegration of S-Monel nodule after etching with dilute HNO_3.

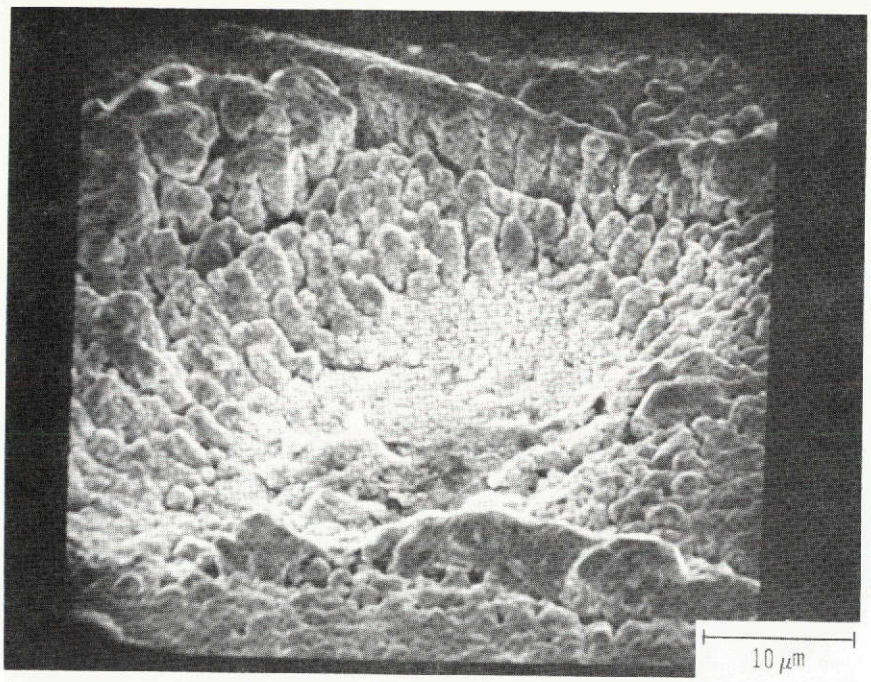

Figure 13. - Removal of nodule-head by chemical etching.

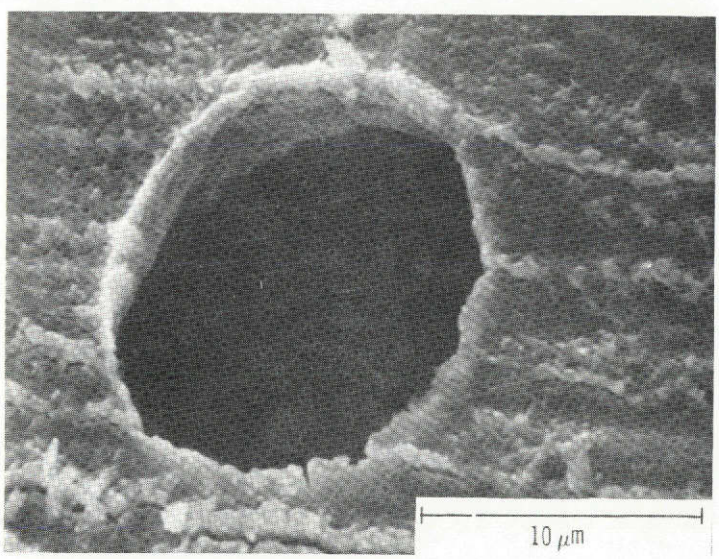

Figure 14. - Complete removal of nodule by etching.

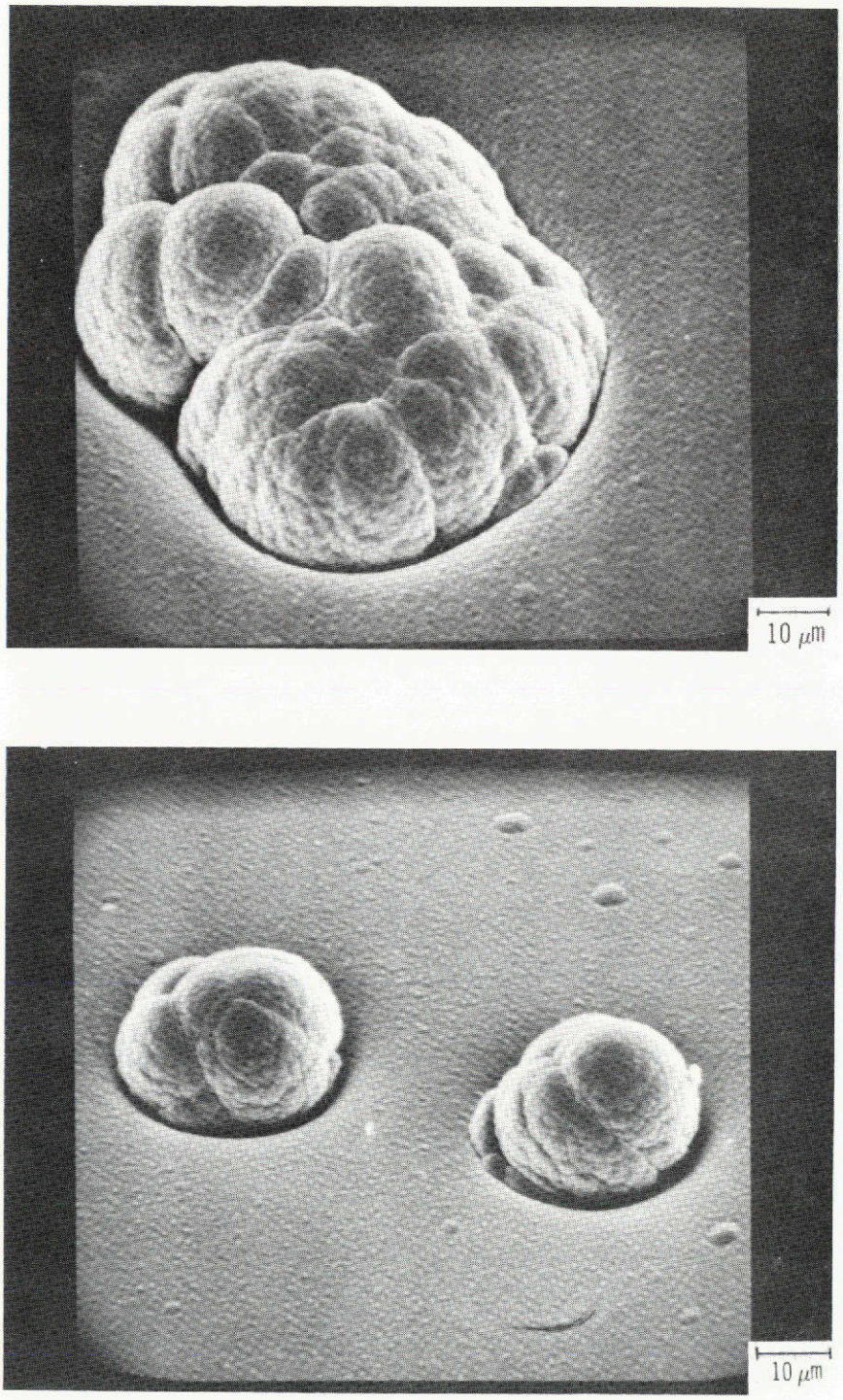

Figure 15. - Surface outgrowths with typical cauliflower structures in sputtered S-Monel on brass.

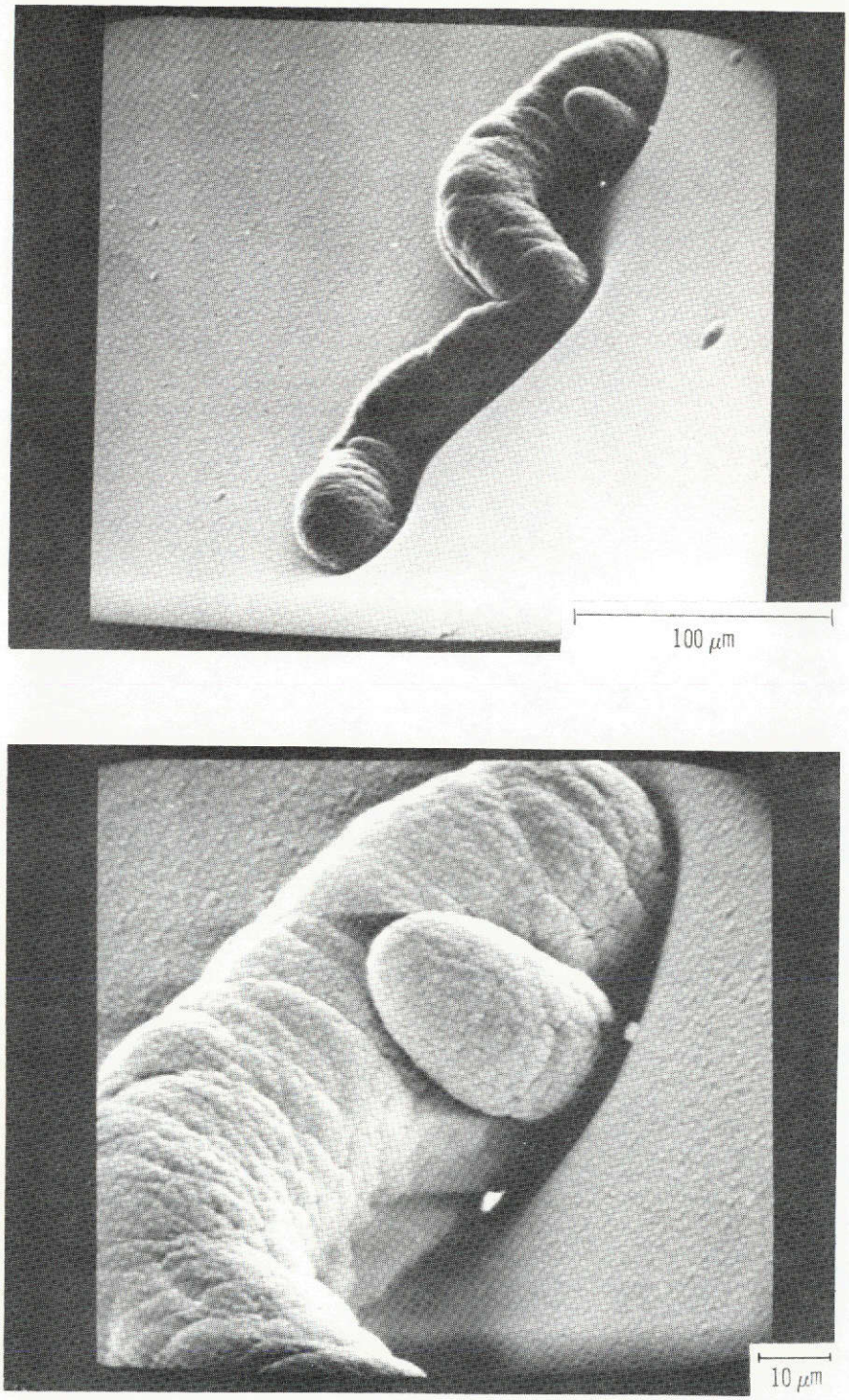

Figure 16. - Surface outgrowth of wormlike structure in sputtered S-Monel on brass.

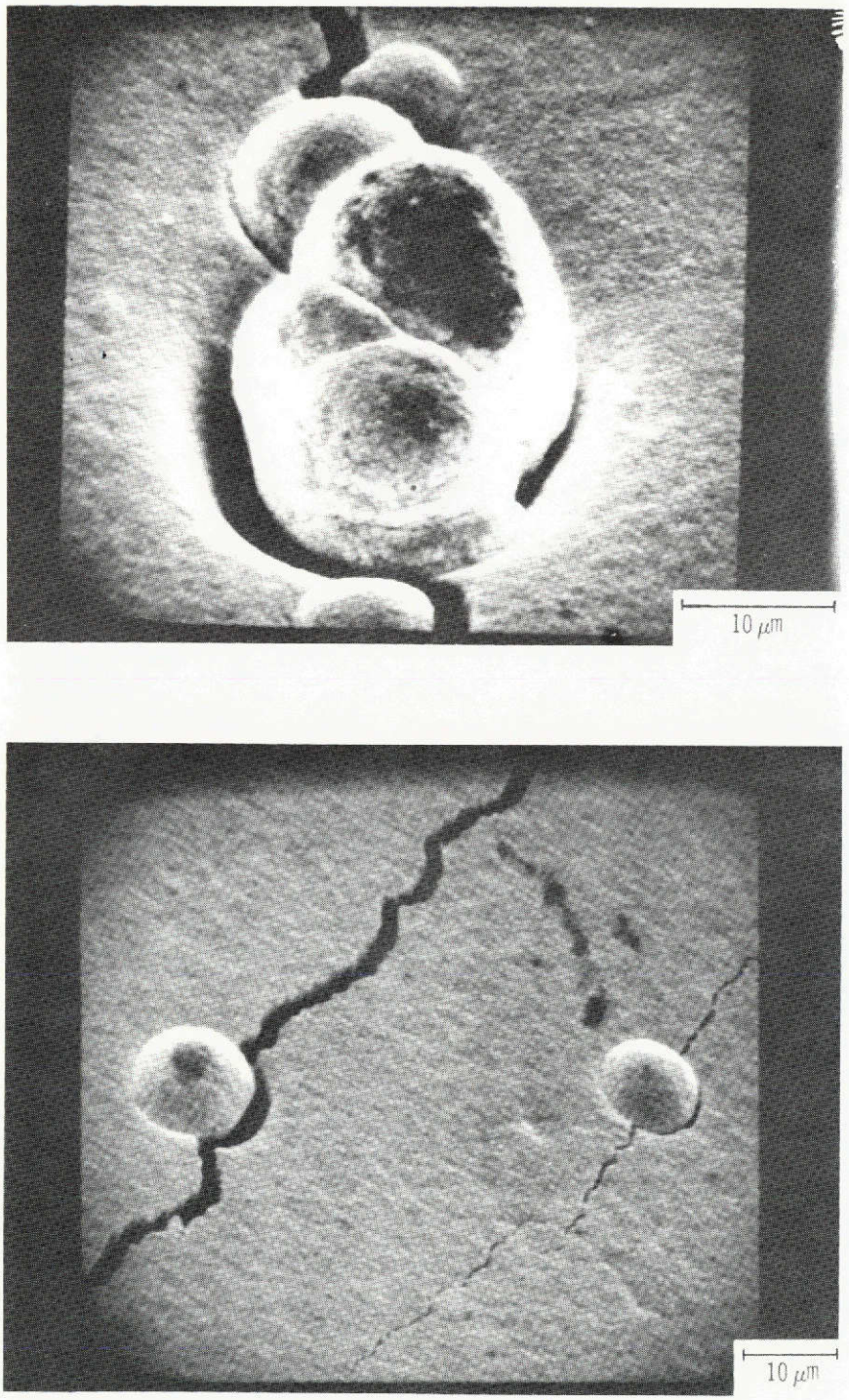

Figure 17. - Cracking around nodule after bending of sputtered S-Monel film.

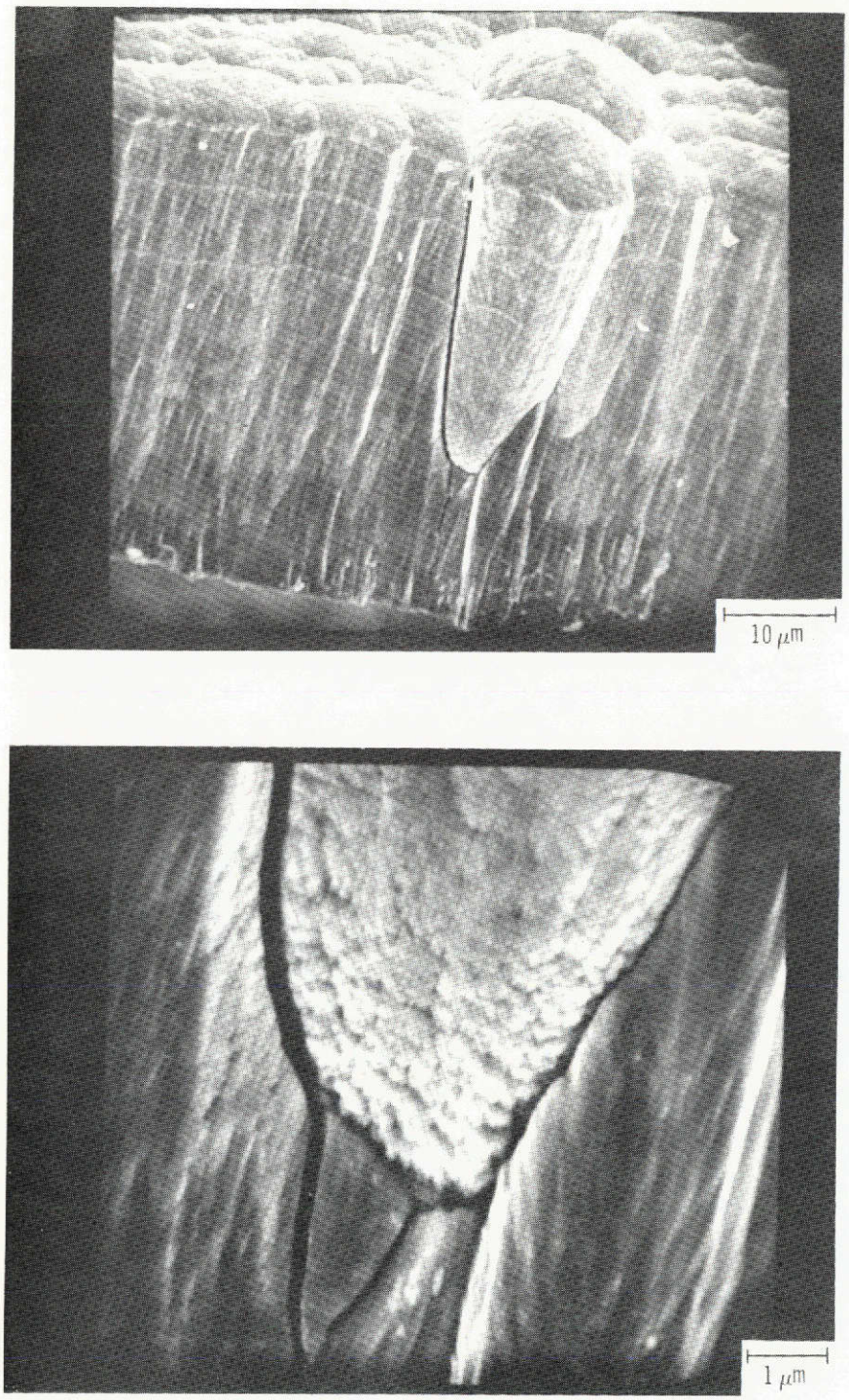

Figure 18. - Cracking around the nodule boundary and in the coating.

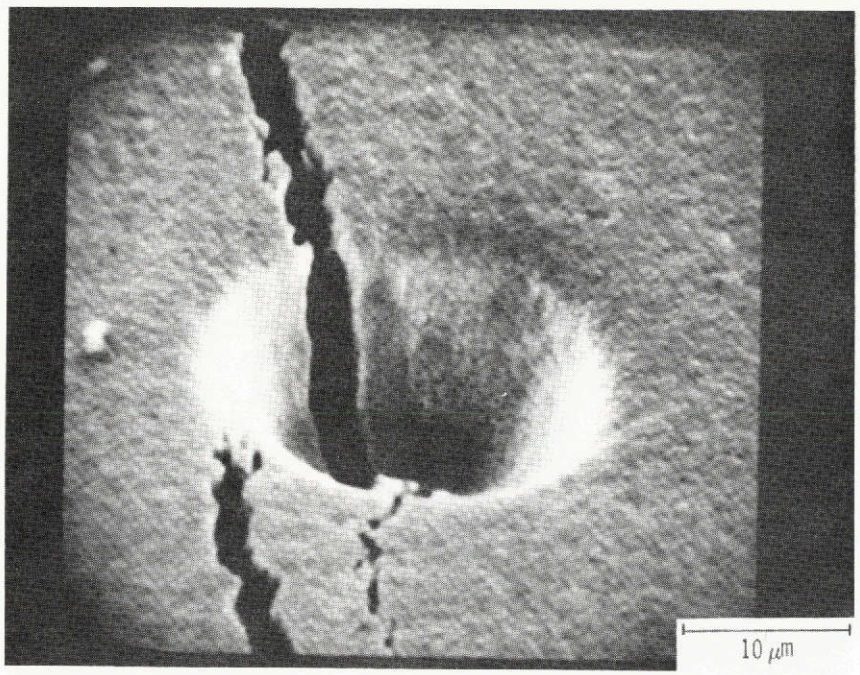

(a) Surface of cavity.

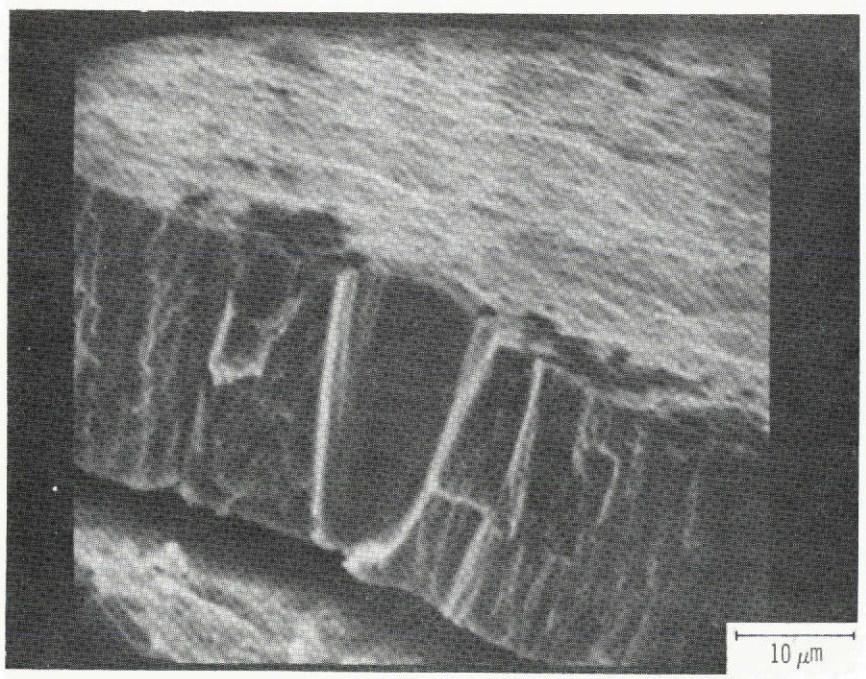

(b) Cross section of cavity.

Figure 19. - Cavity in S-Monel left by ejected nodule.